

# Lyapunov-Based $\mathcal{L}_2$ -Stable PI-Like Control of a Four-Wheel Independently Driven and Steered Robot

Branimir Ćaran<sup>1</sup>, Vladimir Milić<sup>1</sup>, and Bojan Jerbić<sup>1,2</sup>

**Abstract**—In this letter, Lyapunov-based synthesis of a PI-like controller is proposed for  $\mathcal{L}_2$ -stable motion control of an independently driven and steered four-wheel mobile robot. An explicit, structurally verified model is used to enable systematic controller design with stability and performance guarantees suitable for real-time operation. A Lyapunov function is constructed to yield explicit bounds and  $\mathcal{L}_2$  stability results, supporting feedback synthesis that reduces configuration dependent effects. The resulting control law maintains a PI-like form suitable for standard embedded implementation while preserving rigorous stability properties. Effectiveness and robustness are demonstrated experimentally on a real four-wheel mobile robot platform.

**Index Terms**—Wheeled Robots, Motion Control, Robust Control,  $\mathcal{L}_2$  Stability, Lyapunov Function.

## I. INTRODUCTION

Four-wheeled mobile robots with independent steering and drive are attractive for operation in dynamically changing environments due to high manoeuvrability and actuation redundancy. These capabilities have motivated substantial research on this class of robots, leading to a variety of control strategies; see, for example, [1]–[8]. However, this configuration also introduces a nontrivial control problem: how to achieve robust trajectory tracking in the presence of configuration-dependent unmodelled effects, such as friction variations, gravity-related effects during vertical surface operation, and adhesion/contact phenomena, while consistently accounting for the underlying dynamics (i.e., real forces, moments, and constraints) within a unified control framework. In this context, a Lyapunov function is constructed in this work to provide explicit conditions for  $\mathcal{L}_2$  stability, enabling the systematic synthesis of robust feedback loops for such platforms.

In wheeled robot control, passivity-based design offers an energy consistent framework for establishing closed-loop stability, and it is particularly suitable when robustness is desired. A combination of passivity-based modelling and  $\mathcal{L}_2$ -gain robustness analysis has been demonstrated on mobile robot platforms in [9], while related stability and robustness perspectives have been further developed in [10]–[12]. These approaches typically yield constructive stability criteria but may still rely on assumptions that are difficult to guarantee

<sup>1</sup>Authors are with the Faculty of Mechanical Engineering and Naval Architecture, University of Zagreb, Zagreb HR-10000, Croatia  
branimir.caran@fsb.unizg.hr

<sup>2</sup>Bojan Jerbić is with Croatian Academy of Sciences and Arts, Zagreb 10000, Croatia.

This work was supported by Regional Centre of Excellence for Robotic Technology (CRTA), funded by the ERDF fund.

in practice. Robustness against unknown but bounded disturbances has also been addressed within structured control designs for wheeled robots, including settings where constraints and uncertainty must be handled explicitly [13].

In addition, adaptive and sliding-mode methodologies have been used to attenuate disturbances and faults, including finite-time convergence claims under specific modelling premises [14], [15]. Furthermore, related principles and methodologies to those used to solve control problems in autonomous road vehicles can be applied to control four-wheeled mobile robots, for example, approaches published in [16]–[18].

However,  $\mathcal{L}_2$ -based robust control of independently steered and driven four-wheeled robots with a supporting theory and comprehensive experimental validation remains unaddressed.

This work addresses robust motion control of a four-wheeled robot with independent steering and drive under modelling mismatch and external perturbations. For systematic stability analysis, properties of the dynamic model are derived in a form suited for constructive Lyapunov design, yielding explicit stability conditions and energy-based performance bounds. Uncertainties are modelled as algebraic state-dependent terms (with no internal dynamics) and are assumed to be bounded by a constant plus a term proportional to velocity.

A control architecture where an outer kinematic loop generates feasible motion references for an inner dynamic loop at the actuator level, is adopted. The inner loop uses proportional-integral (PI) control with a feedforward term to compensate nominal dynamics, while PI reduces steady-state errors and uncertainties. The closed loop preserves passivity consistent behaviour and guarantees robustness via an  $\mathcal{L}_2$ -gain characterization under bounded disturbances and modelling errors.

Unlike existing PI or passivity-based controllers, the proposed framework provides explicit  $\mathcal{L}_2$ -gain bounds with respect to lumped configuration-dependent uncertainties, while keeping a PI structure suitable for embedded implementation. To the authors' knowledge, this combination of (i) velocity-space modelling, (ii) explicit residual bounds enabling constructive gain tuning, and (iii) experimental validation on vertical surfaces has not been previously reported for four-wheel independently driven and steered robots.

The main contributions are summarized as follows:

- A mathematical model in the velocity space is derived and shown to satisfy key structural properties, including passivity and uniform spectral bounds. A residual dynamics formulation with explicit uncertainty bounds then enables direct  $\mathcal{L}_2$ -stable synthesis for robust trajectory tracking.

- A PI-like controller with feedforward compensation is designed which ensures robust stability, while Lyapunov analysis provides an explicit  $\mathcal{L}_2$ -gain bound and a constructive tuning rule.
- The control strategy is experimentally validated on an independently steered and driven four-wheeled robot on horizontal and vertical surfaces. Robust trajectory tracking is demonstrated under disturbances, unmodelled nonlinearities, and varying contact effects.

The rest of the letter is organized as follows. The model and its properties are presented in Section II. The controller design and main analysis results are given in Section III. Experimental results are reported in Section IV, followed by concluding remarks in Section V.

## II. MATHEMATICAL MODEL AND PROPERTIES

### A. Kinematics

The complete kinematics of an independently steered and driven four-wheeled mobile robot are available in [1], [19], [20]. Assuming rolling without lateral slip and under the symmetric-model assumptions of [21], equal wheel velocities and parallel steering of the front and rear wheel pairs yield the compact representation shown in Fig. 1.

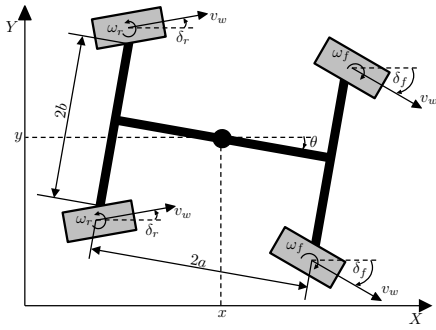


Fig. 1. Mobile robot schematics.

The kinematics are written as

$$\dot{\mathbf{q}} = \mathbf{J}(\mathbf{q})\mathbf{v}, \quad (1)$$

with  $\mathbf{q} = [x \ y \ \theta \ \varphi \ \delta_f \ \delta_r]^T \in \mathbb{R}^6$ ,  $\mathbf{v} = [v_w \ \omega_f \ \omega_r]^T \in \mathbb{R}^3$ , and  $\mathbf{J}(\mathbf{q}) \in \mathbb{R}^{6 \times 3}$  given by

$$\mathbf{J}(\mathbf{q}) = \begin{bmatrix} \frac{1}{2}(\cos(\delta_f + \theta) + \cos(\delta_r + \theta)) & 0 & 0 \\ \frac{1}{2}(\sin(\delta_f + \theta) + \sin(\delta_r + \theta)) & 0 & 0 \\ A(\sin(\delta_f) - \sin(\delta_r)) & 0 & 0 \\ r^{-1} & 0 & 0 \\ 0 & 1 & 0 \\ 0 & 0 & 1 \end{bmatrix}, \quad (2)$$

where  $x, y$  denote the planar position,  $\theta$  the heading,  $\varphi$  the wheel spin angle,  $v_w$  the wheel tangential velocity,  $\delta_f, \omega_f, \delta_r$  and  $\omega_r$  the front/rear steering angles and rates, and  $r$  the wheel radius. Moreover,  $A = a/(2a^2 + b^2)$ , with  $a$  and  $b$  the longitudinal and lateral distances from the centroid to each wheel (half wheelbase and half track width, Fig. 1).

### B. Dynamics

The dynamics are obtained from the Lagrange equations. For the considered simplified symmetric robot system, the kinetic energy is  $T = (m(\dot{x}^2 + \dot{y}^2) + I\dot{\theta}^2 + 4I\dot{\varphi}^2 + 2I_\delta\dot{\delta}_f^2 + 2I_\delta\dot{\delta}_r^2)/2$ , where  $m = m_b + 4m_w$  and  $I = I_\theta + 4m_w(a^2 + b^2)$  denote the total mass and yaw inertia, respectively, while  $I_\varphi$  and  $I_\delta$  denote the wheel-spin and steering inertias. Note that the factors  $4I_\varphi$  and  $2I_\delta$  appear because  $\varphi$  is shared by all four wheels, while  $\delta_f$  and  $\delta_r$  are each shared by two steerable wheels (front and rear), respectively.

The control inputs are grouped as  $\boldsymbol{\tau} = [\tau_w \ \tau_f \ \tau_r]^T \in \mathbb{R}^3$ , with average torques defined by  $\tau_w = \frac{1}{4}\sum_{i=1}^4\tau_{di}$ ,  $\tau_f = (\tau_{s1} + \tau_{s4})/2$ ,  $\tau_r = (\tau_{s2} + \tau_{s3})/2$ , where  $\tau_{di}$  and  $\tau_{si}$  denote the drive and steering torques, respectively.

Using the previous definitions, the constrained dynamics are written as

$$\begin{aligned} \mathbf{M}(\mathbf{q})\ddot{\mathbf{q}} + \mathbf{C}(\mathbf{q}, \dot{\mathbf{q}})\dot{\mathbf{q}} &= \mathbf{B}(\mathbf{q})\boldsymbol{\tau} - \mathbf{f}(\mathbf{q}, \dot{\mathbf{q}}) + \mathbf{A}^T(\mathbf{q})\boldsymbol{\lambda}, \\ \mathbf{A}(\mathbf{q})\dot{\mathbf{q}} &= \mathbf{0}, \end{aligned} \quad (3)$$

where  $\mathbf{M}(\mathbf{q}) \in \mathbb{R}^{6 \times 6}$  is the inertia matrix,  $\mathbf{C}(\mathbf{q}, \dot{\mathbf{q}}) \in \mathbb{R}^{6 \times 6}$  is the Coriolis and centripetal matrix, and  $\mathbf{B}(\mathbf{q}) \in \mathbb{R}^{6 \times 3}$  is the input matrix. The elements of these matrices are as follows:  $\mathbf{M}(\mathbf{q}) = \text{diag}(m, m, I, 4I_\varphi, 2I_\delta, 2I_\delta)$ ,  $\mathbf{C}(\mathbf{q}, \dot{\mathbf{q}}) = \mathbf{0}$  and

$$\mathbf{B}(\mathbf{q}) = \begin{bmatrix} \frac{2}{r}(\cos(\delta_f + \theta) + \cos(\delta_r + \theta)) & 0 & 0 \\ \frac{2}{r}(\sin(\delta_f + \theta) + \sin(\delta_r + \theta)) & 0 & 0 \\ \frac{2a}{r}(\sin(\delta_f) - \sin(\delta_r)) & 0 & 0 \\ 4 & 0 & 0 \\ 0 & 2 & 0 \\ 0 & 0 & 2 \end{bmatrix}. \quad (4)$$

In (3), the constraint matrix  $\mathbf{A}(\mathbf{q}) \in \mathbb{R}^{3 \times 6}$  is

$$\mathbf{A}(\mathbf{q}) = \begin{bmatrix} a_1 & -a_2 & 0 & 0 & 0 & 0 \\ a_3 & 0 & -a_2 & 0 & 0 & 0 \\ 0 & a_3 & -a_1 & 0 & 0 & 0 \end{bmatrix}, \quad (5)$$

with  $a_1 = (\sin(\delta_f + \theta) + \sin(\delta_r + \theta))/2$ ,  $a_2 = (\cos(\delta_f + \theta) + \cos(\delta_r + \theta))/2$ ,  $a_3 = A(\sin(\delta_f) - \sin(\delta_r))$  and  $\boldsymbol{\lambda} \in \mathbb{R}^3$  is the vector of Lagrange multipliers.

*Remark 1:* To obtain the compact kinematic model (1), mathematical simplifications are introduced, yielding a constraint matrix  $\mathbf{A}(\mathbf{q})$  that satisfies  $\mathbf{A}(\mathbf{q})\mathbf{J}(\mathbf{q}) = \mathbf{0}$ , which is required to express (3) in a control-oriented form (see, e.g., [22], [23]). Consequently,  $\mathbf{A}(\mathbf{q})$  captures both the physical Pfaffian nonholonomic constraints (rolling without slipping) and a mathematically induced constraint as the left nullspace complement of  $\mathbf{J}(\mathbf{q})$ .

The vector  $\mathbf{f}(\mathbf{q}, \dot{\mathbf{q}}) \in \mathbb{R}^6$  collects unknown effects and the following assumption is introduced.

*Assumption 1:* Let  $\mathbf{f}(\mathbf{q}, \dot{\mathbf{q}})$  in (3) represent unknown but bounded effects that depend on the current states and velocities and do not introduce additional internal dynamics. The uncertainty is assumed to act on all coordinates, i.e.  $\mathbf{f}(\mathbf{q}, \dot{\mathbf{q}}) = [f_x \ f_y \ f_\theta \ f_\varphi \ f_{\delta_f} \ f_{\delta_r}]^T$ , and each component is bounded as  $|f_k(\mathbf{q}, \dot{\mathbf{q}})| \leq g_k(\mathbf{q}) + h_k(\mathbf{q})|\dot{k}|$  for  $k \in \{x, y, \theta, \varphi, \delta_f, \delta_r\}$ .

On a compact set  $\mathcal{X} \subset \mathbb{R}^6$ , define uniform bounds  $c_k := \sup_{\mathbf{q} \in \mathcal{X}} g_k(\mathbf{q})$ ,  $d_k := \sup_{\mathbf{q} \in \mathcal{X}} h_k(\mathbf{q})$ , which imply

$$\|\mathbf{f}\| \leq \|\mathbf{c}\| + \|\mathbf{d}\| \|\dot{\mathbf{q}}\|, \quad (6)$$

with  $\mathbf{c} = [c_x \ c_y \ c_\theta \ c_\varphi \ c_{\delta_f} \ c_{\delta_r}]^T$  and  $\mathbf{d} = [d_x \ d_y \ d_\theta \ d_\varphi \ d_{\delta_f} \ d_{\delta_r}]^T$ . Furthermore,  $\mathbf{f}$  is assumed to be locally Lipschitz. Let  $\mathbf{f} : \mathbb{R}^6 \times \mathbb{R}^6 \rightarrow \mathbb{R}^6$  be  $C^1$  on an open set containing  $\mathcal{X} \times \mathcal{D}$ , where  $\mathcal{X} \subset \mathbb{R}^6$  and  $\mathcal{D} \subset \mathbb{R}^6$  are compact. Then, with the induced spectral norm,  $L_{f_1} := \sup_{\mathbf{q}, \dot{\mathbf{q}} \in \mathcal{X} \times \mathcal{D}} \|\partial \mathbf{f} / \partial \mathbf{q}\| < \infty$  and  $L_{f_2} := \sup_{\mathbf{q}, \dot{\mathbf{q}} \in \mathcal{X} \times \mathcal{D}} \|\partial \mathbf{f} / \partial \dot{\mathbf{q}}\| < \infty$ , and hence  $\|\partial \mathbf{f} / \partial \mathbf{q}\| \leq L_{f_1}$ ,  $\|\partial \mathbf{f} / \partial \dot{\mathbf{q}}\| \leq L_{f_2} \ \forall \mathbf{q}, \dot{\mathbf{q}} \in \mathcal{X} \times \mathcal{D}$ .

For instance, unmodelled friction effects, gravity-related effects (during vertical surface operation), and adhesion/contact phenomena may be lumped into  $\mathbf{f}(\mathbf{q}, \dot{\mathbf{q}})$  and treated as bounded disturbances on the operating set.

Following [14], [15], [22]–[24], substituting (1) and its derivative  $\ddot{\mathbf{q}} = \mathbf{J}(\mathbf{q})\mathbf{v} + \mathbf{J}(\mathbf{q})\dot{\mathbf{v}}$  into (3), then multiplying by  $\mathbf{J}^T(\mathbf{q})$  and taking into account that  $\mathbf{J}^T(\mathbf{q})\mathbf{A}^T(\mathbf{q}) = \mathbf{0}$  finally yields

$$\tilde{\mathbf{M}}(\mathbf{q})\dot{\mathbf{v}} + \tilde{\mathbf{C}}(\mathbf{q}, \dot{\mathbf{q}})\mathbf{v} = \tilde{\mathbf{B}}(\mathbf{q})\boldsymbol{\tau} - \tilde{\mathbf{f}}(\mathbf{q}, \mathbf{v}), \quad (7)$$

where the reduced matrices and uncertainty term are  $\tilde{\mathbf{M}}(\mathbf{q}) = \mathbf{J}^T(\mathbf{q})\mathbf{M}(\mathbf{q})\mathbf{J}(\mathbf{q}) = \text{diag}(\tilde{M}_{11}, 2I_\delta, 2I_\delta)$ ,  $\tilde{\mathbf{C}}(\mathbf{q}, \dot{\mathbf{q}}) = \mathbf{J}^T(\mathbf{q})\mathbf{M}(\mathbf{q})\mathbf{J}(\mathbf{q}) = \text{diag}(\tilde{C}_{11}, 0, 0)$ ,  $\tilde{\mathbf{B}}(\mathbf{q}) = \mathbf{J}^T(\mathbf{q})\mathbf{B}(\mathbf{q}) = \text{diag}(\tilde{B}_{11}, 2, 2)$  and  $\tilde{\mathbf{f}}(\mathbf{q}, \mathbf{v}) = \mathbf{J}^T(\mathbf{q})\mathbf{f}(\mathbf{q}, \mathbf{J}(\mathbf{q})\mathbf{v}) = [\tilde{f} \ f_{\delta_f} \ f_{\delta_r}]^T$  with

$$\begin{aligned} \tilde{M}_{11} &= \frac{4I_\varphi}{r^2} + \frac{m}{2}(1 + \cos(\delta_f - \delta_r)) \\ &\quad + IA^2(\sin(\delta_f) - \sin(\delta_r))^2, \end{aligned} \quad (8)$$

$$\begin{aligned} \tilde{C}_{11} &= IA^2(\sin(\delta_f) - \sin(\delta_r))(\cos(\delta_f)\dot{\delta}_f - \cos(\delta_r)\dot{\delta}_r) \\ &\quad - \frac{m}{4}\sin(\delta_f - \delta_r)(\dot{\delta}_f - \dot{\delta}_r), \end{aligned} \quad (9)$$

$$\begin{aligned} \tilde{B}_{11} &= \frac{1}{r}[2(1 + \cos(\delta_f - \delta_r)) \\ &\quad + \frac{a^2}{a^2 + b^2}(\sin(\delta_f) - \sin(\delta_r))^2 + 4], \end{aligned} \quad (10)$$

$$\begin{aligned} \tilde{f} &= \frac{1}{2}(\cos(\delta_f + \theta) + \cos(\delta_r + \theta))f_x + \frac{1}{2}(\sin(\delta_f + \theta) \\ &\quad + \sin(\delta_r + \theta))f_y + A(\sin(\delta_f) - \sin(\delta_r))f_\theta + \frac{1}{r}f_\varphi. \end{aligned} \quad (11)$$

The dynamics (7) satisfy the following structural properties, which enable Lyapunov-based analysis and explicit  $\mathcal{L}_2$ -stability conditions.

*Property 1:* The matrix  $\tilde{\mathbf{M}}(\mathbf{q})$  is symmetric positive-definite for all configurations of  $\mathbf{q}$ .

*Proof:* The proof is straightforward and is omitted for brevity.  $\blacksquare$

*Property 2:* There exist positive constants  $a_1$  and  $a_2$  such that  $a_1\|\mathbf{z}\|^2 \leq \mathbf{z}^T \tilde{\mathbf{M}}(\mathbf{q}) \mathbf{z} \leq a_2\|\mathbf{z}\|^2$ ,  $\forall \mathbf{z} \in \mathbb{R}^3$ .

*Proof:* Since  $\tilde{\mathbf{M}}(\mathbf{q})$  is diagonal, its eigenvalues are  $\tilde{M}_{11}$  and  $2I_\delta$ . Using  $-1 \leq \cos(\delta_f - \delta_r) \leq 1$  and  $0 \leq (\sin(\delta_f) - \sin(\delta_r))^2 \leq 4$  yields  $4I_\varphi/r^2 \leq \tilde{M}_{11} \leq 4I_\varphi/r^2 + m + 4IA^2$ . Therefore uniform (i.e. configuration independent) bounds may be chosen as  $a_1 = \lambda_{\min}\{\tilde{\mathbf{M}}\} = \min\{4I_\varphi/r^2, 2I_\delta\}$ ,

$a_2 = \lambda_{\max}\{\tilde{\mathbf{M}}\} = \max\{4I_\varphi/r^2 + m + 4IA^2, 2I_\delta\}$ . The quantities  $\lambda_{\min}\{\cdot\}$  and  $\lambda_{\max}\{\cdot\}$  denote, respectively, the smallest and largest eigenvalues of the symmetric positive-definite matrix.  $\blacksquare$

*Property 3:* The matrix  $\dot{\tilde{\mathbf{M}}}(\mathbf{q}) - 2\tilde{\mathbf{C}}(\mathbf{q}, \dot{\mathbf{q}})$  is skew-symmetric.

*Proof:* The proof follows by direct differentiation and subtraction and is omitted for brevity.  $\blacksquare$

*Remark 2:* Properties 1 and 3 imply the energy-balance identity  $\dot{\tilde{\mathbf{M}}}(\mathbf{q}) = \tilde{\mathbf{C}}(\mathbf{q}, \dot{\mathbf{q}}) + \tilde{\mathbf{C}}(\mathbf{q}, \dot{\mathbf{q}})^T$  and hence  $\tilde{\mathbf{C}}(\mathbf{q}, \dot{\mathbf{q}}) = \frac{1}{2}\dot{\tilde{\mathbf{M}}}(\mathbf{q})$ .

*Property 4:* There exists positive constant  $b_c$  such that for all  $\mathbf{v} = [v_w \ \omega_f \ \omega_r]^T = [v_w \ \dot{\delta}_f \ \dot{\delta}_r]^T$ ,  $\|\tilde{\mathbf{C}}(\mathbf{q}, \dot{\mathbf{q}})\mathbf{v}\| \leq b_c\|\mathbf{v}\|^2$ .

*Proof:* Since  $\tilde{\mathbf{C}}(\mathbf{q}, \dot{\mathbf{q}})$  has only the (1, 1) entry and thus  $\|\tilde{\mathbf{C}}(\mathbf{q}, \dot{\mathbf{q}})\mathbf{v}\| = |\tilde{C}_{11}v_w|$ . Using  $|\sin(\cdot)| \leq 1$  and  $|\cos(\cdot)| \leq 1$  gives

$$\begin{aligned} |\tilde{C}_{11}| &\leq 2IA^2(|\dot{\delta}_f| + |\dot{\delta}_r|)(|\sin(\delta_f)| + |\sin(\delta_r)|) \\ &\quad + \frac{m}{4}(|\dot{\delta}_f| + |\dot{\delta}_r|) = \left(2IA^2 + \frac{m}{4}\right)(|\dot{\delta}_f| + |\dot{\delta}_r|). \end{aligned} \quad (12)$$

Consequently,

$$\begin{aligned} \|\tilde{\mathbf{C}}(\mathbf{q}, \dot{\mathbf{q}})\mathbf{v}\| &\leq \left(2IA^2 + \frac{m}{4}\right)|v_w|(|\dot{\delta}_f| + |\dot{\delta}_r|) \\ &\leq \left(2IA^2 + \frac{m}{4}\right)\left(\frac{1}{2}v_w^2 + \dot{\delta}_f^2 + \dot{\delta}_r^2\right) \leq b_c\|\mathbf{v}\|^2, \end{aligned} \quad (13)$$

and an explicit choice is  $b_c = 2IA^2 + m/4$ .  $\blacksquare$

*Property 5:* The matrix  $\tilde{\mathbf{B}}(\mathbf{q})$  is invertible for all configurations.

*Proof:* The proof is straightforward since  $\tilde{\mathbf{B}}(\mathbf{q})$  is diagonal with strictly positive diagonal entries, and is omitted for brevity.  $\blacksquare$

*Property 6:* If there exist nonnegative constants  $c_k$  and  $d_k$  defined in Assumption 1 such that (6) is satisfied then

$$\|\tilde{\mathbf{f}}\| \leq \tilde{c} + \tilde{d}\|\mathbf{v}\|, \quad (14)$$

with  $\tilde{c} = \sigma_J\|\mathbf{c}\|$  and  $\tilde{d} = \sigma_J^2\|\mathbf{d}\|$  where  $\mathbf{c}$  and  $\mathbf{d}$  are as in (6). Here  $\sigma_J$  denotes the uniform induced gain of (2) under the weighted norm.

*Proof:* A weighted norm on the configuration derivative space is introduced as  $\|\dot{\mathbf{q}}\|_W = \sqrt{\dot{\mathbf{q}}^T \mathbf{W} \dot{\mathbf{q}}}$  with  $\mathbf{W} = \text{diag}(1, 1, 1, r^2, 1, 1)$  which measures  $r\dot{\varphi}$  instead of  $\dot{\varphi}$  and thus avoids the amplification induced by  $\dot{\varphi} = v_w/r$ . The compatible induced matrix norm of (2) is defined by  $\|\mathbf{J}\|_W := \sup_{\mathbf{v} \neq 0} \|\mathbf{J}\mathbf{v}\|_W / \|\mathbf{v}\| = \sqrt{\lambda_{\max}\{\mathbf{J}^T \mathbf{W} \mathbf{J}\}}$ , and the corresponding uniform bound is set as  $\sigma_J := \sup_{\mathbf{q} \in \mathcal{X}} \|\mathbf{J}\|_W$ . By definition,  $\tilde{\mathbf{f}}(\mathbf{q}, \mathbf{v}) = \mathbf{J}^T(\mathbf{q})\mathbf{f}(\mathbf{q}, \mathbf{J}(\mathbf{q})\mathbf{v})$ . Using submultiplicativity and (6),  $\|\tilde{\mathbf{f}}\| \leq \|\mathbf{J}^T\|_W \|\mathbf{f}\| \leq \|\mathbf{J}\|_W (\|\mathbf{c}\| + \|\mathbf{d}\| \|\dot{\mathbf{q}}\|_W)$ , and since  $\|\dot{\mathbf{q}}\|_W = \|\mathbf{J}\mathbf{v}\|_W \leq \|\mathbf{J}\|_W \|\mathbf{v}\|$ , it follows that  $\|\tilde{\mathbf{f}}\| \leq \sigma_J\|\mathbf{c}\| + \sigma_J^2\|\mathbf{d}\| \|\mathbf{v}\|$ , which yields (14) with  $\tilde{c} = \sigma_J\|\mathbf{c}\|$  and  $\tilde{d} = \sigma_J^2\|\mathbf{d}\|$ . Moreover, the induced gain in satisfies  $\|\mathbf{J}\|_W = \sqrt{\lambda_{\max}\{\mathbf{J}^T \mathbf{W} \mathbf{J}\}} = \max\{\sqrt{S}, 1\}$ , where  $S = (1 + \cos(\delta_f - \delta_r))/2 + A^2(\sin(\delta_f) - \sin(\delta_r))^2 + 1$ . Therefore, using  $(1 + \cos(\cdot))/2 \leq 1$  and  $(\sin(\delta_f) - \sin(\delta_r))^2 \leq 4$ , the uniform bound becomes  $\sigma_J \leq \sqrt{2 + 4A^2}$ . Note that the bound  $\sigma_J$  is interpreted in the scaled coordinate metric induced by the preceding norm definition. Accordingly, the factor  $A$  enters

the induced-gain bound through this scaling so that  $\sigma_J$  remains dimensionally consistent.  $\blacksquare$

The aforementioned properties provide explicit estimates of  $a_1, a_2, b_c, \tilde{c}, \tilde{d}$  and  $\sigma_J$  in terms of robot parameters, which supports explicit controller-tuning conditions for guaranteeing  $\mathcal{L}_2$  stability.

### III. CONTROLLER DESIGN BASED ON LYAPUNOV STABILITY ANALYSIS

This section focuses on inner-loop tracking of (7) with a PI controller and feedforward, and quantifies robustness to bounded unmodelled nonlinearities (Property 6) via a finite  $\mathcal{L}_2$ -gain from  $\tilde{\mathbf{f}}$  to  $\mathbf{e}_v$ . A brief outline of the virtual kinematic controller used to generate the references is also provided.

#### A. Control problem formulation

1) *Virtual kinematic controller*: Let the reference pose be  $x_d(t), y_d(t), \theta_d(t)$  with desired forward velocity  $v_t(t) > 0$  and yaw-rate  $\omega_d(t) = \dot{\theta}_d(t)$ . Define the tracking errors  $e_x = (x_d - x) \cos(\theta) + (y_d - y) \sin(\theta)$ ,  $e_y = -(x_d - x) \sin(\theta) + (y_d - y) \cos(\theta)$ ,  $e_\theta = \theta_d - \theta$ . A stabilizing kinematic tracking law is  $v_{w,d} = v_t \cos(e_\theta) + k_x e_x$  and  $\omega_{virt} = \omega_d + k_\theta e_\theta + k_y v_t e_y$  with  $k_x, k_y, k_\theta > 0$  [25]. If the inner loop enforces  $v_w \approx v_{w,d}$  and  $\theta \approx \omega_{virt}$ , the tracking error dynamics are (locally) exponentially stable and input-to-state stable [25].

Using (1)-(2),  $\dot{\theta} = v_w A(\sin(\delta_f) - \sin(\delta_r))$ . Following [20], initialize steering from the reference motion and errors. Let  $\theta_d = \text{atan2}(\dot{y}_d, \dot{x}_d)$ ,  $v_t = \sqrt{\dot{x}_d^2 + \dot{y}_d^2}$ ,  $a_f = a_r = v_t \cos(\theta_d) + k_x e_x$ ,  $b_f = v_t \sin(\theta_d) + k_y v_t e_y - k_\theta a e_\theta$ ,  $b_r = v_t \sin(\theta_d) + k_y v_t e_y + k_\theta a e_\theta$ , and  $\delta_{f,d} = \text{atan2}(b_f, a_f)$ ,  $\delta_{r,d} = \text{atan2}(b_r, a_r)$ , where  $a$  is the centroid-to-axle distance (Fig. 1). Define the normalized yaw demand  $s = \omega_{virt}/(A \text{sgn}_\varepsilon(v_{w,d}) \max(|v_{w,d}|, \varepsilon_v))$  with  $\varepsilon_v > 0$  and  $\text{sgn}_\varepsilon(0) = 1$ . Enforce  $\sin(\delta_{f,d}) - \sin(\delta_{r,d}) \approx s$  via  $d_{req} = s - (\sin(\delta_{f,d}) - \sin(\delta_{r,d}))$ ,  $\hat{s}_f = \sin(\delta_{f,d}) + d_{req}/2$ ,  $\hat{s}_r = \sin(\delta_{r,d}) - d_{req}/2$ , followed by saturation  $\hat{s}_{(\cdot)} \in [-1, 1]$  and angle unwrapping, equivalently,  $\delta_{f,d} = \text{atan2}(\hat{s}_f, \sqrt{1 - \hat{s}_f^2})$ ,  $\delta_{r,d} = \text{atan2}(\hat{s}_r, \sqrt{1 - \hat{s}_r^2})$  (respecting  $|\delta_{(\cdot),d}| \leq \delta_{max}$ , if saturation occurs, reduce  $\omega_{virt}$  accordingly).

Track  $\delta_{f,d}$  and  $\delta_{r,d}$  with first-order laws  $\omega_{f,d} = -k_\delta(\delta_f - \delta_{f,d})$  and  $\omega_{r,d} = -k_\delta(\delta_r - \delta_{r,d})$ , with  $k_\delta > 0$  and  $|\omega_{(\cdot),d}| \leq \dot{\delta}_{max}$ .

2) *Dynamic controller*: A PI-type control law with feed-forward compensation is considered in the following form

$$\begin{aligned} \tau &= \tilde{\mathbf{B}}^{-1}(\mathbf{q}) \left( -\mathbf{K}_P \mathbf{e}_v - \mathbf{K}_I \boldsymbol{\eta} \right. \\ &\quad \left. + \tilde{\mathbf{M}}(\mathbf{q}_d) \dot{\mathbf{v}}_d + \tilde{\mathbf{C}}(\mathbf{q}_d, \dot{\mathbf{q}}_d) \mathbf{v}_d \right), \end{aligned} \quad (15)$$

$$\dot{\boldsymbol{\eta}} = \mathbf{e}_v, \quad (16)$$

where  $\mathbf{v}_d = [v_{w,d} \ \omega_{f,d} \ \omega_{r,d}]^T$  is the desired reference velocity generated by the previously described virtual kinematic controller,  $\mathbf{e}_v = \mathbf{v} - \mathbf{v}_d$  is the velocity error, and  $\boldsymbol{\eta} \in \mathbb{R}^3$  is the integral state. The gain matrices  $\mathbf{K}_P$  and  $\mathbf{K}_I$  are diagonal and positive definite.

The robust control objective is stated as follows.

*Problem 1:* Given the dynamic model (7) satisfying Properties 1-5 with bounded uncertainty  $\tilde{\mathbf{f}}(\mathbf{q}, \mathbf{v})$  satisfying Property 6, and the reference velocity  $\mathbf{v}_d(t)$  generated by the virtual kinematic controller, determine diagonal positive-definite gains  $\mathbf{K}_P$  and  $\mathbf{K}_I$  in (15) such that the closed-loop system is robustly  $\mathcal{L}_2$ -stable with respect to  $\mathbf{e}_v = \mathbf{v} - \mathbf{v}_d$  and has finite  $\mathcal{L}_2$ -gain from  $\tilde{\mathbf{f}}$  to  $\mathbf{e}_v$ .

*Remark 3:* Property 6 models  $\tilde{\mathbf{f}}(\mathbf{q}, \mathbf{v})$  as a bounded memoryless nonlinearity, so the stated  $\mathcal{L}_2$ -gain is interpreted as a uniform finite-gain energy estimate along closed-loop trajectories.

The overall control system for the considered mobile robot is shown in Fig. 2.

#### B. Stability analysis

1) *Residual dynamics*: For a given desired velocity  $\mathbf{v}_d(t)$  with associated desired state  $\mathbf{q}_d(t)$  robot system dynamics (7) can be rewritten in the following form

$$\begin{aligned} \tilde{\mathbf{M}}(\mathbf{q}) \dot{\mathbf{e}}_v + \tilde{\mathbf{C}}(\mathbf{q}, \dot{\mathbf{q}}) \mathbf{e}_v + \mathbf{r} &= \tilde{\mathbf{B}}(\mathbf{q}) \boldsymbol{\tau} - \mathbf{u}_d \\ &\quad + \tilde{\mathbf{f}}(\mathbf{q}, \mathbf{v}_d) - \tilde{\mathbf{f}}(\mathbf{q}, \mathbf{v}), \end{aligned} \quad (17)$$

where  $\mathbf{r} = \tilde{\mathbf{M}}(\mathbf{q}) \dot{\mathbf{v}}_d + \tilde{\mathbf{C}}(\mathbf{q}, \dot{\mathbf{q}}) \mathbf{v}_d + \tilde{\mathbf{f}}(\mathbf{q}, \mathbf{v}_d) - \mathbf{u}_d$  is residual and  $\mathbf{u}_d = \tilde{\mathbf{M}}(\mathbf{q}_d) \dot{\mathbf{v}}_d + \tilde{\mathbf{C}}(\mathbf{q}_d, \dot{\mathbf{q}}_d) \mathbf{v}_d$ .

Assume  $\delta_f, \delta_r \in \mathcal{D}_\delta$  and  $|\dot{\delta}_f|, |\dot{\delta}_r| \leq \dot{\delta}_{max}$ . Let  $V_d := \sup_t \|\mathbf{v}_d(t)\|$  and  $A_d := \sup_t \|\dot{\mathbf{v}}_d(t)\|$ .

*Property 7:* There exist positive Lipschitz constants  $L_M, L_{C_1}, L_{C_2}$  such that

$$\|\tilde{\mathbf{M}}(\mathbf{q}_1) - \tilde{\mathbf{M}}(\mathbf{q}_2)\| \leq L_M \|\mathbf{q}_1 - \mathbf{q}_2\|, \quad (18)$$

$$\begin{aligned} \|\tilde{\mathbf{C}}(\mathbf{q}_1, \dot{\mathbf{q}}_1) - \tilde{\mathbf{C}}(\mathbf{q}_2, \dot{\mathbf{q}}_2)\| &\leq L_{C_1} \|\mathbf{q}_1 - \mathbf{q}_2\| \\ &\quad + L_{C_2} \|\dot{\mathbf{q}}_1 - \dot{\mathbf{q}}_2\|, \end{aligned} \quad (19)$$

for all  $\mathbf{q}_1, \dot{\mathbf{q}}_1, \mathbf{q}_2, \dot{\mathbf{q}}_2$  in the operating domain.

*Proof:* Since  $\tilde{\mathbf{M}}(\mathbf{q})$  and  $\tilde{\mathbf{C}}(\mathbf{q}, \dot{\mathbf{q}})$  are diagonal, the bounds follow from mean-value arguments applied to  $\tilde{M}_{11}$  and  $\tilde{C}_{11}$ . Hence,  $L_M := \sup_{\delta_f, \delta_r \in \mathcal{D}_\delta} \|[\partial \tilde{M}_{11}/\partial \delta_f \ \partial \tilde{M}_{11}/\partial \delta_r]^T\|$ ,  $L_{C_1} := \sup_{\delta_f, \delta_r \in \mathcal{D}_\delta, |\dot{\delta}_{(\cdot)}| \leq \dot{\delta}_{max}} \|[\partial \tilde{C}_{11}/\partial \delta_f \ \partial \tilde{C}_{11}/\partial \delta_r]^T\|$  and  $L_{C_2} := \sup_{\delta_f, \delta_r \in \mathcal{D}_\delta} \|[\partial \tilde{C}_{11}/\partial \dot{\delta}_f \ \partial \tilde{C}_{11}/\partial \dot{\delta}_r]^T\|$ . Using  $|\sin(\cdot)| \leq 1$ ,  $|\cos(\cdot)| \leq 1$  and  $|\sin(\delta_f) - \sin(\delta_r)| \leq 2$ ,  $|\dot{\delta}_{(\cdot)}| \leq \dot{\delta}_{max}$ , one obtains  $L_M \leq \sqrt{2}(m/2 + 4IA^2)$ ,  $L_{C_1} \leq \sqrt{2}(m/4 + 4IA^2)\dot{\delta}_{max}$  and  $L_{C_2} \leq \sqrt{2}(m/4 + 2IA^2)$ .  $\blacksquare$

*Property 8:* There exists a constant  $d_v > 0$  such that

$$\|\tilde{\mathbf{f}}(\mathbf{q}, \mathbf{v}_d) - \tilde{\mathbf{f}}(\mathbf{q}, \mathbf{v})\| \leq d_v \|\mathbf{v} - \mathbf{v}_d\|. \quad (20)$$

An explicit choice is  $d_v := \sup_{\mathbf{q}, \dot{\mathbf{q}} \in \mathcal{X} \times \mathcal{D}} \|\mathbf{J}(\mathbf{q})^T \frac{\partial \mathbf{f}}{\partial \dot{\mathbf{q}}} \mathbf{J}(\mathbf{q})\|$  and the computable conservative bound  $d_v \leq (\sup_{\mathbf{q} \in \mathcal{X}} \|\mathbf{J}(\mathbf{q})\|)^2 (\sup_{\mathbf{q}, \dot{\mathbf{q}} \in \mathcal{X} \times \mathcal{D}} \|\partial \mathbf{f} / \partial \dot{\mathbf{q}}\|) \leq \sigma_J^2 L_{f_2}$ , where  $\mathbf{f}$  satisfies Assumption 1,  $\mathbf{J}$  is Jacobian (2),  $\sigma_J$  is bounded as in Property 6, and  $L_{f_2}$  is defined as in Assumption 1. Under Assumption 1,  $L_{f_2}$  is an upper bound on the induced spectral norm of  $\partial \mathbf{f} / \partial \dot{\mathbf{q}}$  over  $\mathcal{X} \times \mathcal{D}$ .

*Proof:* Fix  $\mathbf{q} \in \mathcal{X} \subset \mathbb{R}^6$  and define  $\mathbf{G}(\mathbf{q}, \mathbf{v}) := \tilde{\mathbf{f}}(\mathbf{q}, \mathbf{v}) = \mathbf{J}^T(\mathbf{q}) \mathbf{f}(\mathbf{q}, \mathbf{J}(\mathbf{q}) \mathbf{v})$ . By Assumption 1,  $\mathbf{G}$  is  $C^1$  and the chain rule yields  $\frac{\partial \mathbf{G}}{\partial \mathbf{v}} = \mathbf{J}^T(\mathbf{q}) \frac{\partial \mathbf{f}}{\partial \dot{\mathbf{q}}} \mathbf{J}(\mathbf{q})$ . By the mean-value theorem, there exists  $\boldsymbol{\xi}$  on the line segment between  $\mathbf{v}$  and  $\mathbf{v}_d$  such that  $\|\tilde{\mathbf{f}}(\mathbf{q}, \mathbf{v}_d) - \tilde{\mathbf{f}}(\mathbf{q}, \mathbf{v})\| = \|\mathbf{G}(\mathbf{q}, \mathbf{v}_d) - \mathbf{G}(\mathbf{q}, \mathbf{v})\| \leq$

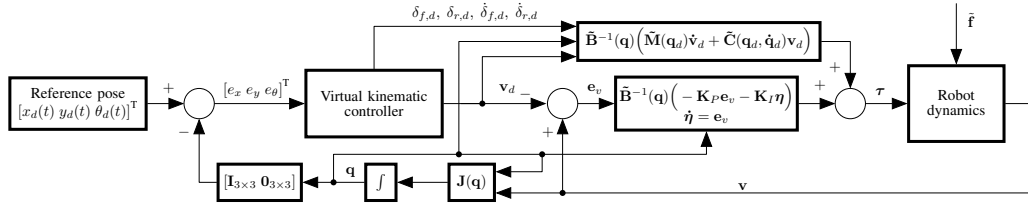


Fig. 2. Block diagram of the overall control system for the considered mobile robot.

$\|\frac{\partial \mathbf{G}}{\partial \mathbf{v}}|_{\mathbf{v}=\xi}\| \|\mathbf{v} - \mathbf{v}_d\|$ . Taking the supremum over  $\mathbf{q}, \xi \in \mathcal{X}$  yields the definition of  $d_v$ . Finally, using submultiplicativity of the induced operator norm,  $\|\mathbf{J}^T(\mathbf{q}) \frac{\partial \mathbf{f}}{\partial \mathbf{q}} \mathbf{J}(\mathbf{q})\| \leq \|\mathbf{J}(\mathbf{q})\|^2 \|\frac{\partial \mathbf{f}}{\partial \mathbf{q}}\|$ , and taking suprema over  $\mathcal{X}$  gives a bound on  $d_v$ . ■

*Property 9:* For all  $\mathbf{q}, \mathbf{q}_d, \mathbf{v}, \mathbf{v}_d \in \mathcal{X} \times \mathcal{X} \times \mathbb{R}^3 \times \mathbb{R}^3$ , kinematic difference is bounded with

$$\|\dot{\mathbf{q}} - \dot{\mathbf{q}}_d\| \leq \sigma_J \|\mathbf{e}_v\| + \sigma_{\partial J} V_d \|\mathbf{q} - \mathbf{q}_d\|, \quad (21)$$

where  $\sigma_J$  is bounded as in Property 6, and  $\sigma_{\partial J} \leq \sqrt{3/2 + 2A^2}$  where  $A$  is defined in (2).

*Proof:* From (1),  $\dot{\mathbf{q}} - \dot{\mathbf{q}}_d = \mathbf{J}(\mathbf{q})\mathbf{v} - \mathbf{J}(\mathbf{q}_d)\mathbf{v}_d = \mathbf{J}(\mathbf{q})\mathbf{e}_v + (\mathbf{J}(\mathbf{q}) - \mathbf{J}(\mathbf{q}_d))\mathbf{v}_d$ . Taking the Euclidean norm and using the triangle inequality,  $\|\dot{\mathbf{q}} - \dot{\mathbf{q}}_d\| \leq \|\mathbf{J}(\mathbf{q})\mathbf{e}_v\| + \|(\mathbf{J}(\mathbf{q}) - \mathbf{J}(\mathbf{q}_d))\mathbf{v}_d\| \leq \|\mathbf{J}(\mathbf{q})\|\|\mathbf{e}_v\| + \|\mathbf{J}(\mathbf{q}) - \mathbf{J}(\mathbf{q}_d)\|V_d$ . For the first term, use  $\|\mathbf{J}(\mathbf{q})\| \leq \sigma_J$  to bound  $\|\mathbf{J}(\mathbf{q})\mathbf{e}_v\|$ . For the second term, by the mean-value estimate for matrix valued  $C^1$  maps (Fréchet differentiability) there exists  $\xi$  on the segment joining  $\mathbf{q}$  and  $\mathbf{q}_d$  such that  $\|\mathbf{J}(\mathbf{q}) - \mathbf{J}(\mathbf{q}_d)\| \leq \sup_{\mathbf{q} \in [\mathbf{q}, \mathbf{q}_d]} \|\partial \mathbf{J}(\xi)/\partial \mathbf{q}\| \|\mathbf{q} - \mathbf{q}_d\| \leq \sigma_{\partial J} \|\mathbf{q} - \mathbf{q}_d\|$ . Substituting these bounds yields (21).

For deriving the bound of  $\sigma_{\partial J}$ , the submultiplicativity, definition of the Fréchet derivative (the linear approximation) of a matrix valued function and its induced operator norm, triangle inequality and Cauchy-Schwarz-based quadratic bound are used, and based on elements of Jacobian matrix in (2), yields  $\sigma_{\partial J} := \sup_{\mathbf{q} \in [\mathbf{q}, \mathbf{q}_d]} \|\partial \mathbf{J}/\partial \mathbf{q}\| = \sup_{\|\Delta \mathbf{q}\|=1} \|\sum_k \mathbf{J}_{k,k} \Delta k\| \leq (\sum_k \|\mathbf{J}_{k,k}\|^2)^{1/2} \leq \sqrt{3/2 + 2A^2}$ , for  $k \in \{\theta, \delta_f, \delta_r\}$ , where  $\mathbf{J}_{k,k}$  denotes the directional (Fréchet) derivative of  $\mathbf{J}$  evaluated at  $\mathbf{q}$  along the  $k$ -th coordinate direction of the configuration space. ■

Using Properties 6, 7 and 9, the residual  $\mathbf{r} = \tilde{\mathbf{M}}(\mathbf{q})\dot{\mathbf{v}}_d + \tilde{\mathbf{C}}(\mathbf{q}, \dot{\mathbf{q}})\mathbf{v}_d + \tilde{\mathbf{f}}(\mathbf{q}, \mathbf{v}_d) - \mathbf{u}_d$  with  $\mathbf{u}_d = \tilde{\mathbf{M}}(\mathbf{q}_d)\dot{\mathbf{v}}_d + \tilde{\mathbf{C}}(\mathbf{q}_d, \dot{\mathbf{q}}_d)\mathbf{v}_d$  from (17) satisfies

$$\|\mathbf{r}\| \leq A_q \|\mathbf{q} - \mathbf{q}_d\| + A_v \|\mathbf{e}_v\| + A_c. \quad (22)$$

where  $A_q = L_M \|\dot{\mathbf{v}}_d\| + L_{C_1} \|\mathbf{v}_d\| + L_{C_2} \sigma_{\partial J} \|\mathbf{v}_d\|^2$ ,  $A_v = L_{C_2} \sigma_J \|\mathbf{v}_d\|$  and  $A_c = \tilde{c} + \tilde{d} \|\mathbf{v}_d\|$ . Using  $\|\mathbf{v}_d(t)\| \leq V_d$  and  $\|\dot{\mathbf{v}}_d(t)\| \leq A_d$ , the coefficients in (22) can be chosen time-invariant as

$$\begin{aligned} A_q &= L_M A_d + L_{C_1} V_d + L_{C_2} \sigma_{\partial J} V_d^2, \\ A_v &= L_{C_2} \sigma_J V_d, \quad A_c = \tilde{c} + \tilde{d} V_d. \end{aligned} \quad (23)$$

2) *Derivation of a Lyapunov function candidate:* A Lyapunov function construction similar to [26], [27] is used.

Substituting (15) into (17) yields

$$\begin{aligned} \tilde{\mathbf{M}}(\mathbf{q})\dot{\mathbf{e}}_v + \tilde{\mathbf{C}}(\mathbf{q}, \dot{\mathbf{q}})\mathbf{e}_v + \mathbf{r} = \\ -\mathbf{K}_P \mathbf{e}_v - \mathbf{K}_I \eta + \tilde{\mathbf{f}}(\mathbf{q}, \mathbf{v}_d) - \tilde{\mathbf{f}}(\mathbf{q}, \mathbf{v}). \end{aligned} \quad (24)$$

Multiply (24) by  $\mathbf{e}_v^T$  and using the identities  $\mathbf{e}_v^T \tilde{\mathbf{M}}(\mathbf{q}) \dot{\mathbf{e}}_v = \frac{d}{dt} \left( \frac{1}{2} \mathbf{e}_v^T \tilde{\mathbf{M}}(\mathbf{q}) \mathbf{e}_v \right) - \frac{1}{2} \mathbf{e}_v^T \dot{\tilde{\mathbf{M}}}(\mathbf{q}) \mathbf{e}_v$  and  $\mathbf{e}_v^T \mathbf{K}_I \eta = \frac{d}{dt} \left( \frac{1}{2} \mathbf{e}_v^T \mathbf{K}_I \eta \right)$ , together with  $\mathbf{K}_I = \mathbf{K}_I^T$  and Property 3, yields

$$\begin{aligned} \frac{d}{dt} \left( \frac{1}{2} \mathbf{e}_v^T \tilde{\mathbf{M}}(\mathbf{q}) \mathbf{e}_v + \frac{1}{2} \eta^T \mathbf{K}_I \eta \right) = \\ -\mathbf{e}_v^T \mathbf{K}_P \mathbf{e}_v + \mathbf{e}_v^T \left( \tilde{\mathbf{f}}(\mathbf{q}, \mathbf{v}_d) - \tilde{\mathbf{f}}(\mathbf{q}, \mathbf{v}) \right). \end{aligned} \quad (25)$$

The left-hand side of (25) defines the Lyapunov function (i.e. storage function), and the right-hand side provides its time derivative.

3)  *$\mathcal{L}_2$  stability conditions:* Using standard output strict passivity arguments,  $\mathcal{L}_2$  stability and gain conditions are obtained. The definitions of output strict passivity,  $\mathcal{L}_2$  stability, and  $\mathcal{L}_2$ -gain used in this analysis can be found, for example, in [28].

*Corollary 1 (Quadratic bounds on the storage function):* Let the storage function be the Lyapunov function on the left-hand side of (25):

$$V = \frac{1}{2} \mathbf{e}_v^T \tilde{\mathbf{M}}(\mathbf{q}) \mathbf{e}_v + \frac{1}{2} \eta^T \mathbf{K}_I \eta. \quad (26)$$

By Property 2 and  $\mathbf{K}_I = \mathbf{K}_I^T > \mathbf{0}$ , for all admissible  $\mathbf{q}$  the following bounds hold  $V \geq (a_1 \|\mathbf{e}_v\|^2 + \lambda_{\min}\{\mathbf{K}_I\} \|\eta\|^2)/2$  and  $V \leq (a_2 \|\mathbf{e}_v\|^2 + \lambda_{\max}\{\mathbf{K}_I\} \|\eta\|^2)/2$ . Thus,  $V$  is positive definite and radially unbounded in  $[\mathbf{e}_v^T \ \eta^T]^T$  on the operating set.

*Proposition 1 (Negative semidefiniteness of the Lyapunov function derivative):* Let the Lyapunov derivative be the right-hand side of (25). Suppose (22) with (23) and (20) hold. If there exists  $\varepsilon > 0$  such that

$$\lambda_{\min}\{\mathbf{K}_P\} > d_v + A_v + \varepsilon, \quad (27)$$

then, along the trajectories of (24), the Lyapunov derivative satisfies

$$\begin{aligned} \dot{V} \leq & -(\lambda_{\min}\{\mathbf{K}_P\} - d_v - A_v - \varepsilon) \|\mathbf{e}_v\|^2 \\ & + \frac{A_q^2}{2\varepsilon} \|\mathbf{q} - \mathbf{q}_d\|^2 + \frac{A_c^2}{2\varepsilon}, \end{aligned} \quad (28)$$

and hence  $\dot{V}$  is negative semidefinite in the nominal case, and negative semidefinite whenever  $\|\mathbf{e}_v\| \geq R$ , where  $R$  depends on  $A_q$ ,  $A_c$  and  $\varepsilon$ . Here, the nominal case refers to the idealized situation in which  $\tilde{\mathbf{f}} \equiv 0$ , the reference is exactly matched  $\mathbf{q} \equiv \mathbf{q}_d$ , and the residual term  $\mathbf{r}$  vanishes, i.e.  $A_c = 0$ .

*Proof:* From the right-hand side of (25),  $\dot{V} = -\mathbf{e}_v^T \mathbf{K}_P \mathbf{e}_v - \mathbf{e}_v^T \mathbf{r} + \mathbf{e}_v^T (\tilde{\mathbf{f}}(\mathbf{q}, \mathbf{v}_d) - \tilde{\mathbf{f}}(\mathbf{q}, \mathbf{v}))$ . Bound each term: (i)  $-\mathbf{e}_v^T \mathbf{K}_P \mathbf{e}_v \leq -\lambda_{\min}\{\mathbf{K}_P\} \|\mathbf{e}_v\|^2$ , (ii) by Cauchy-Schwarz

and (22),  $-\mathbf{e}_v^T \mathbf{r} \leq \|\mathbf{e}_v\| \|\mathbf{r}\| \leq A_v \|\mathbf{e}_v\|^2 + A_q \|\mathbf{e}_v\| \|\mathbf{q} - \mathbf{q}_d\| + A_c \|\mathbf{e}_v\|$ , (iii) by (20),  $\mathbf{e}_v^T (\tilde{\mathbf{f}}(\mathbf{q}, \mathbf{v}_d) - \tilde{\mathbf{f}}(\mathbf{q}, \mathbf{v})) \leq d_v \|\mathbf{e}_v\|^2$ . Combining these estimates yields  $\dot{V} \leq -(\lambda_{\min}\{\mathbf{K}_P\} - A_v - d_v) \|\mathbf{e}_v\|^2 + A_q \|\mathbf{e}_v\| \|\mathbf{q} - \mathbf{q}_d\| + A_c \|\mathbf{e}_v\|$ . Applying Young's inequality with the same  $\varepsilon > 0$  gives  $A_q \|\mathbf{e}_v\| \|\mathbf{q} - \mathbf{q}_d\| \leq \frac{\varepsilon}{2} \|\mathbf{e}_v\|^2 + \frac{A_q^2}{2\varepsilon} \|\mathbf{q} - \mathbf{q}_d\|^2$ ,  $A_c \|\mathbf{e}_v\| \leq \frac{\varepsilon}{2} \|\mathbf{e}_v\|^2 + \frac{A_c^2}{2\varepsilon}$ . Thus  $\dot{V} \leq -(\lambda_{\min}\{\mathbf{K}_P\} - d_v - A_v - \varepsilon) \|\mathbf{e}_v\|^2 + \frac{A_q^2}{2\varepsilon} \|\mathbf{q} - \mathbf{q}_d\|^2 + \frac{A_c^2}{2\varepsilon}$ , which is (28). If  $\mathbf{q} \equiv \mathbf{q}_d$  and  $A_c = 0$ , the last two terms vanish and  $\dot{V} \leq -(\lambda_{\min}\{\mathbf{K}_P\} - d_v - A_v - \varepsilon) \|\mathbf{e}_v\|^2 \leq 0$  by (27). In the general case, write  $\dot{V} \leq -\mu_\varepsilon \|\mathbf{e}_v\|^2 + \rho_\varepsilon$  with  $\mu_\varepsilon = \lambda_{\min}\{\mathbf{K}_P\} - d_v - A_v - \varepsilon > 0$ ,  $\rho_\varepsilon = \frac{A_q^2}{2\varepsilon} \|\mathbf{q} - \mathbf{q}_d\|^2 + \frac{A_c^2}{2\varepsilon}$ , which shows practical negative semidefiniteness outside the ball  $\|\mathbf{e}_v\| \geq \sqrt{\rho_\varepsilon / \mu_\varepsilon}$ . ■

*Remark 4:* Condition (27) requires  $\lambda_{\min}\{\mathbf{K}_P\}$  to dominate  $d_v$  and  $A_v$ , with slack  $\varepsilon$ . The remaining terms enter through  $\rho_\varepsilon$  and decrease with improved kinematic tracking (smaller  $\|\mathbf{q} - \mathbf{q}_d\|$ ) and reduced uncertainty level (smaller  $A_c$ ).

*Remark 5:* The reference generator in subsection III-A1 provides a smooth desired configuration  $\mathbf{q}_d$  and velocity  $\mathbf{v}_d$ . Consequently,  $\|\mathbf{q} - \mathbf{q}_d\|$  in  $\rho(t)$  is proportional to the pose-tracking error and vanishes on the path manifold, tightening the bounds in Proposition 1.

*Proposition 2 (Output strict passivity and finite-gain  $\mathcal{L}_2$  stability):* Consider the closed-loop system under the proposed control law (24) and let the storage function be  $V$  defined in (26). Define the input and output as  $\mathbf{u} = -\tilde{\mathbf{f}}(\mathbf{q}, \mathbf{v})$  and  $\mathbf{y} = \mathbf{e}_v$ , respectively. Assume that the conditions of Assumption 1 and Properties 6 and 8 hold, and that there exists  $\varepsilon > 0$  such that

$$\mu = \lambda_{\min}\{\mathbf{K}_P\} - d_v - A_v - \varepsilon > 0. \quad (29)$$

Then the mapping  $\mathbf{u} \mapsto \mathbf{y}$  is output strictly passive with respect to the supply rate  $\mathbf{y}^T \mathbf{u}$ . Along closed-loop trajectories,

$$\dot{V} \leq \mathbf{y}^T \mathbf{u} - \mu \|\mathbf{y}\|^2 + \rho(t), \quad (30)$$

where  $\rho(t) = \frac{A_q^2}{2\varepsilon} \|\mathbf{q} - \mathbf{q}_d\|^2 + \frac{A_c^2}{2\varepsilon}$ . Moreover, the system is finite-gain  $\mathcal{L}_2$  stable from  $\mathbf{u}$  to  $\mathbf{y}$ , and for any  $T \geq 0$  it holds that

$$\|\mathbf{y}\|_{[0,T]}^2 \leq \frac{1}{\mu^2} \|\mathbf{u}\|_{[0,T]}^2 + \frac{2}{\mu} \left( V(0) + \int_0^T \rho(t) dt \right). \quad (31)$$

Hence, the mapping  $\mathbf{u} \mapsto \mathbf{y}$  is finite-gain  $\mathcal{L}_2$  stable with gain bounded by  $1/\mu$ , with an additive term depending on  $V(0)$  and  $\int_0^T \rho(t) dt$ .

*Proof:* From the right-hand side of (25) one has  $\dot{V} = -\mathbf{e}_v^T \mathbf{K}_P \mathbf{e}_v - \mathbf{e}_v^T \mathbf{r} + \mathbf{e}_v^T \tilde{\mathbf{f}}(\mathbf{q}, \mathbf{v}_d) - \mathbf{e}_v^T \tilde{\mathbf{f}}(\mathbf{q}, \mathbf{v})$ . Using the aforementioned definition of input and output,  $-\mathbf{e}_v^T \tilde{\mathbf{f}}(\mathbf{q}, \mathbf{v}) = \mathbf{y}^T \mathbf{u}$ . The remaining terms are bounded as in Proposition 1 using Property 8 and Young's inequality, yielding (30) with (29). Integrating (30) over  $[0, T]$  gives  $V(T) - V(0) \leq \int_0^T \mathbf{y}^T \mathbf{u} dt - \mu \|\mathbf{y}\|_{[0,T]}^2 + \int_0^T \rho(t) dt$ . Since  $V(T) \geq 0$ , it follows that  $\mu \|\mathbf{y}\|_{[0,T]}^2 \leq \int_0^T \mathbf{y}^T \mathbf{u} dt + V(0) + \int_0^T \rho(t) dt$ . Finally, by Cauchy-Schwarz,  $\int_0^T \mathbf{y}^T \mathbf{u} dt \leq \|\mathbf{y}\|_{[0,T]} \|\mathbf{u}\|_{[0,T]}$ , and applying Young's inequality  $\|\mathbf{y}\|_{[0,T]} \|\mathbf{u}\|_{[0,T]} \leq \frac{\mu}{2} \|\mathbf{y}\|_{[0,T]}^2 + \frac{1}{2\mu} \|\mathbf{u}\|_{[0,T]}^2$  yields (31) (with the additive term scaled by  $2/\mu$ ) after rearranging terms. ■

*Remark 6:* If, instead of  $\mathbf{u} = -\tilde{\mathbf{f}}(\mathbf{q}, \mathbf{v})$  in Proposition 2, the composite input is chosen as follows  $\mathbf{u}_c = -(\tilde{\mathbf{f}}(\mathbf{q}, \mathbf{v}) - \tilde{\mathbf{f}}(\mathbf{q}, \mathbf{v}_d)) - \mathbf{r} = \mathbf{u} + \tilde{\mathbf{f}}(\mathbf{q}, \mathbf{v}_d) - \mathbf{r}$ , then from the right-hand side of (25) it follows that  $\dot{V} = -\mathbf{e}_v^T \mathbf{K}_P \mathbf{e}_v + \mathbf{e}_v^T \mathbf{u}_c \leq \mathbf{e}_v^T \mathbf{u}_c - \lambda_{\min}\{\mathbf{K}_P\} \|\mathbf{e}_v\|^2$ . Hence, the mapping  $\mathbf{u}_c \mapsto \mathbf{e}_v$  is exactly output strictly passive with  $\mu = \lambda_{\min}\{\mathbf{K}_P\}$ , i.e., no  $\rho$  term is required.

*Remark 7:* Since Property 4 holds on the operating set, the sensitivity constant  $L_{C_2}$  entering  $A_v$  and  $A_q$  can be conservatively replaced by  $b_c$  using  $\dot{\mathbf{q}} = \mathbf{J}(\mathbf{q})\mathbf{v}$ , which can reduce conservatism in (22).

#### IV. EXPERIMENTAL VALIDATION

##### A. Experimental set-up

The mobile robot used for experimental validation was originally designed for vertical-surface locomotion and nondestructive testing. Its structure combines carbon-fiber tubes and 3D-printed acrylonitrile styrene acrylate (ASA) components, providing high stiffness at low mass. The robot is actuated by eight DC motors (Dynamixel XH430-W210), with four assigned to wheel steering and four to wheel driving, enabling quasi-omnidirectional motion and stable orientation during vertical operation. Torque-controlled actuation allows high-rate control updates. The hybrid adhesion system consists of an electric ducted fan and a drone-type propulsion unit arranged near the robot's center of gravity. This configuration enhances adhesion and compensates for gravitational effects during vertical motion.

The control system is implemented on an onboard computer running ROS 2, using the `ros2_control` framework to provide a unified velocity control architecture for the driving and steering wheels. Fig. 3 illustrates the experimental configurations of the robot on the vertical test surface and the horizontal test surface.

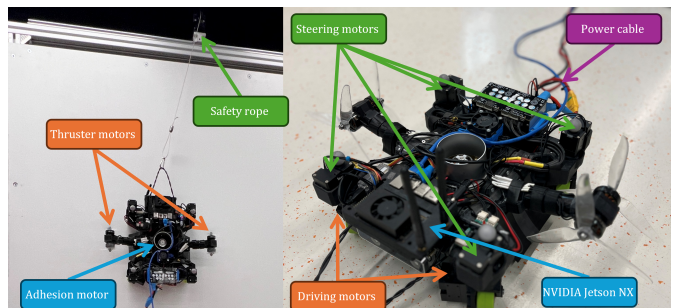


Fig. 3. Experimental setup of the mobile robot on vertical surface (left) and horizontal surface (right)

##### B. Experimental results

Two experimental scenarios are considered: (i) planar flower-trajectory tracking on a horizontal surface with disturbance injection, and (ii) Lissajous-trajectory tracking on a vertical surface under gravity and adhesion-driven contact effects. In the planar case, robustness is assessed by applying external disturbances via thrusters acting against the driving direction, while the adhesion system increases the effective

normal load. In the vertical case, adhesion ensures wall contact and thrusters provide lifting force for gravity compensation, leading to significant disturbances and complex contact effects.

Table I summarizes the physical parameters of the robot. From these values, the gain-selection constants are  $\sigma_J = 4.6640$  (see Property 6),  $L_{C_2} = 1.7479$  kg (see Property 7),  $|v_w| \leq v_{w,max} = 0.13$  m/s,  $|\dot{\delta}_{(.)}| \leq \dot{\delta}_{max} = \pi/2$  rad/s,  $V_d \leq \sqrt{v_{w,max}^2 + 2a^2\dot{\delta}_{max}^2} = 0.2817$  m/s. Here a weighted Euclidean norm is employed, i.e.,  $\|\mathbf{v}_d\|_W^2 = v_{w,d}^2 + (a\dot{\delta}_{f,d})^2 + (a\dot{\delta}_{r,d})^2 \leq v_{w,max}^2 + 2a^2\dot{\delta}_{max}^2$ , thereby ensuring dimensional consistency. Furthermore,  $A_v = 2.2964$  kgm/s (see (23)). Note that  $\dot{\delta}_{max}$  is a steering-reference design limit, not the physical actuator saturation. Hence the manufacturer-declared peak rate ( $\approx 5.24$  rad/s) is not used in gain selection, since the analysis requires a bound consistent with the admissible reference signals.

Viscous friction in the actuation is modelled with coefficient  $b_f = 0.0305$  Nms/rad, which accounts for the motor-reducer losses and the wheel-ground contact effects. Accordingly,  $L_{f_2} = b_f = 0.0305$  Nms/rad (see Assumption 1) and  $d_v = 0.6635$  Nms/rad (see Property 8). Therefore, the sufficient condition for passivity and  $\mathcal{L}_2$ -gain stability requires  $\lambda_{min}\{\mathbf{K}_P\} > d_v + A_v + \varepsilon = 2.9599 + \varepsilon$ , where  $\varepsilon > 0$  is selected according to Proposition 2.

For implementation in current control mode, torque domain gains are mapped using  $K_t = 1.923$  Nm/A. Accordingly, the sufficient condition (27) corresponds to  $\lambda_{min}\{\mathbf{K}_P\} > (d_v + A_v + \varepsilon)/K_t = 1.539 + \varepsilon/K_t$ . Therefore,  $\lambda_{min}\{\mathbf{K}_P\} = 1.563$  is chosen to satisfy (27) (for small  $\varepsilon$ ) and the gains were subsequently fine-tuned to improve the transient response while preserving the inequality, yielding  $\mathbf{K}_P = \text{diag}(1.563 \text{ As/m}, 2.344 \text{ As/rad}, 2.344 \text{ As/rad})$  and  $\mathbf{K}_I = \text{diag}(0.061 \text{ A/m}, 0.092 \text{ A/rad}, 0.092 \text{ A/rad})$ , with  $k_x = k_y = k_\theta = k_\delta = 5 \text{ s}^{-1}$ . The same controller gains are used in both experiments, highlighting robustness of the proposed PI-like inner loop across substantially different disturbance and contact regimes.

Fig. 4a presents results for the flower-shaped trajectory  $x_d(t) = 0.5 \cos(2\pi t/35) \cos(2\pi t/70) + 0.1$ ,  $y_d(t) = 0.5 \cos(2\pi t/35) \sin(2\pi t/70) + 0.2$  and  $\theta_d(t) = \text{atan2}(y_d, \dot{x}_d)$ . The presented results show that the motor torques increase at the presence of the applied disturbances. Despite this transient increase in actuation effort, the velocity tracking performance remains stable, which in turn ensures stable tracking of the kinematic trajectory in the  $x$ - $y$  plane. The observed tracking under increased actuation is consistent with finite-gain  $\mathcal{L}_2$  robustness. It should be emphasized that the reference curves shown in the plots correspond exclusively to the nominal (disturbance-free) trajectory in order to prevent visual ambiguity.

The results of the second experiment, in which the robot moves on a vertical surface, are shown in Fig. 4b. Trajectory used for this experiment is defined as  $x_d(t) = 0.75 \cos(0.1t - \pi/2 + 0.75)$ ,  $y_d(t) = -0.5 \sin(0.2t - \pi)$ , and  $\theta_d(t) = 0.0$ . It should be noted that, in order for the thruster motors to effectively contribute to assisted motion along the vertical surface, it is necessary to maintain a constant orientation

TABLE I  
ROBOT PHYSICAL PARAMETERS.

Parameter	Description	Value
$r$	Wheel radius	0.0254 m
$a$	Half-length of robot body	0.1125 m
$b$	Half-width of robot body	0.1125 m
$m$	Robot mass	3.50 kg
$m_w$	Wheel mass	0.03203 kg
$I_\theta$	Robot yaw inertia	0.03333 kgm <sup>2</sup>
$I_\varphi$	Wheel rotational inertia	$1.03 \times 10^{-5}$ kgm <sup>2</sup>
$I_\delta$	Steering inertia	0.002 kgm <sup>2</sup>
$A$	$a/(2a^2 + b^2)$	2.2222 m <sup>-1</sup>
$I$	$I_\theta + 4m_w(a^2 + b^2)$	0.0365 kgm <sup>2</sup>

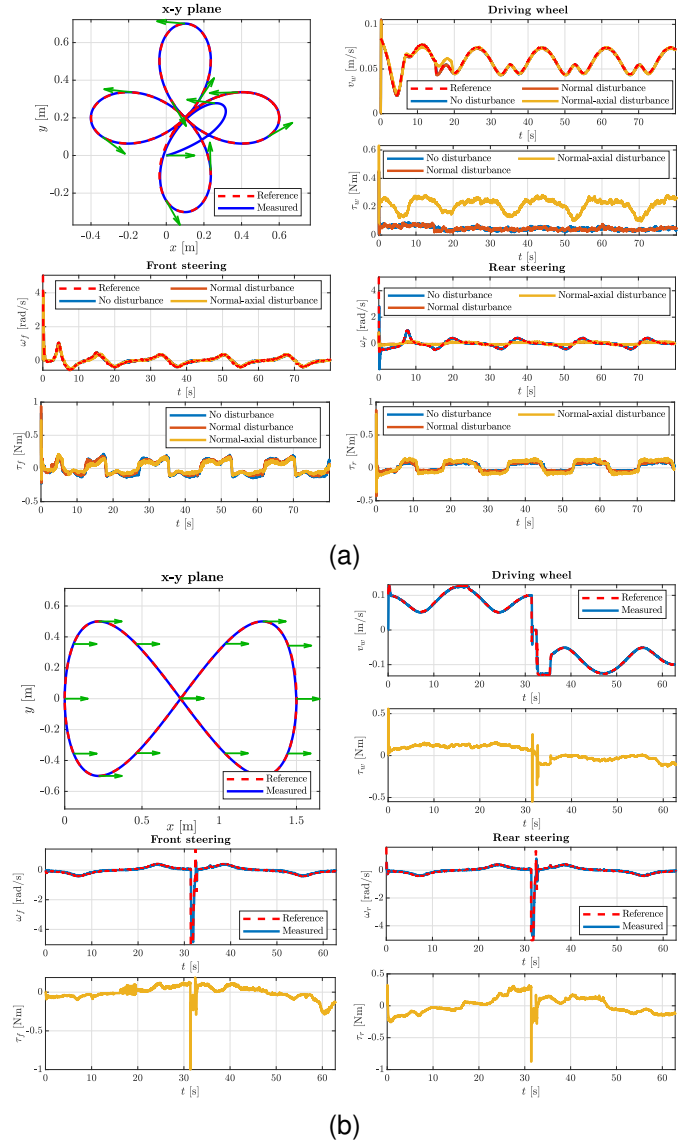


Fig. 4. Experimental results for trajectory tracking: (a) horizontal surface, (b) vertical surface. Green arrows indicate robot orientation.

of the robot,  $\theta_d = 0.0$  rad. In contrast to the planar case, the motor torques remain relatively low, since the adhesion system ensures stable contact with the surface, while the thrusters assist the driven wheels in counteracting gravitational effects during upward motion. Furthermore, it can be observed that during the second part of the trajectory, when the robot

descends along the vertical surface, the motor torques are close to zero, as the actuators primarily operate in a braking regime to maintain accurate trajectory tracking. In both motion phases, the tracking of the reference velocity trajectory, as well as the tracking of the kinematic trajectory in the  $x$ - $y$  plane, remains stable and accurate. Overall, experiments indicate attenuated gravity and contact uncertainties without loss of stability, consistent with a finite  $\mathcal{L}_2$ -gain to tracking error.

Short peaks in  $\omega_{(.)}$  are observed and are attributed to reference-generation transients of the virtual kinematic controller, i.e., abrupt changes in the mapped steering reference  $\delta_{(.)}$  at initialization and during mode transitions due to steering-angle unwrapping and sign changes in the commanded longitudinal velocity (e.g., at the top of the Lissajous trajectory). Hence, these peaks are regarded as brief reference-mapping events rather than sustained steering-rate demands, and  $\dot{\delta}_{max} = \pi/2 \text{ rad/s}$  is adopted as a conservative bound for steady tracking.

A video demonstrating the conducted experiments is provided in the supplementary material.

## V. CONCLUSION

This letter proposed a Lyapunov based PI-like control framework for robust trajectory tracking of an independently steered and driven four-wheel mobile robot. Exploiting structural properties of a velocity-space dynamic model, sufficient conditions for robust  $\mathcal{L}_2$ -stability and finite  $\mathcal{L}_2$ -gain were derived via constructive Lyapunov analysis, yielding a simple PI-like controller with feedforward compensation suitable for real-time implementation.

The approach was experimentally validated on a real robot under diverse operating conditions, including horizontal motion with disturbances and vertical motion with gravity, adhesion, and complex contact effects. The results demonstrate stable closed-loop behaviour and accurate trajectory tracking, confirming the practical effectiveness of the proposed framework.

## REFERENCES

- [1] C.-C. Tsai, C.-C. Hung, C.-F. Mao, H.-S. Wu, and C.-H. Chen, "Fuzzy neural LSTM-RBLS for fractional-order PID sliding-mode motion control of autonomous mobile robots with four ISI wheels," *International Journal of Fuzzy Systems*, vol. 27, no. 7, pp. 2195–2213, 2025.
- [2] M. Cipriano, G. Oriolo, and A. Cherubini, "Singularity-free trajectory tracking for steerable wheeled mobile robots," *IEEE Robotics and Automation Letters*, vol. 10, no. 6, pp. 6199–6206, 2025.
- [3] R. R. Shamshiri, A. Azimi, M. Behjati, A. Ghasemzadeh, V. Dworak, C. Weltzien, K. Karydis, and F. A. A. Cheein, "Online path tracking with an integrated  $\mathcal{H}_\infty$  robust adaptive controller for a double-ackermann steering robot for orchard waypoint navigation," *International Journal of Intelligent Robotics and Applications*, vol. 9, no. 1, pp. 257–277, 2025.
- [4] X. Zhang, Y. Huang, S. Wang, W. Meng, G. Li, and Y. Xie, "Motion planning and tracking control of a four-wheel independently driven steered mobile robot with multiple maneuvering modes," *Frontiers of Mechanical Engineering*, vol. 16, no. 3, pp. 504–527, 2021.
- [5] R. Sonker and A. Dutta, "Adding terrain height to improve model learning for path tracking on uneven terrain by a four wheel robot," *IEEE Robotics and Automation Letters*, vol. 6, no. 1, pp. 239–246, 2021.
- [6] L. Jiang, S. Wang, Y. Xie, J. Meng, S. Zheng, X. Zhang, and H. Wu, "Anti-disturbance direct yaw moment control of a four-wheeled autonomous mobile robot," *IEEE Access*, vol. 8, pp. 174654–174666, 2020.
- [7] M. Sorour, A. Cherubini, P. Fraisse, and R. Passama, "Motion discontinuity-robust controller for steerable mobile robots," *IEEE Robotics and Automation Letters*, vol. 2, no. 2, pp. 452–459, 2017.
- [8] T.-H. S. Li, M.-H. Lee, C.-W. Lin, G.-H. Liou, and W.-C. Chen, "Design of autonomous and manual driving system for 4WIS4WID vehicle," *IEEE Access*, vol. 4, pp. 2256–2271, 2016.
- [9] B. Morales, F. Roberti, J. M. Toibero, and R. Carelli, "Passivity based visual servoing of mobile robots with dynamics compensation," *Mechatronics*, vol. 22, no. 4, pp. 481–490, 2012.
- [10] V. H. Andaluz, F. Roberti, L. Salinas, J. M. Toibero, and R. Carelli, "Passivity-based visual feedback control with dynamic compensation of mobile manipulators: Stability and  $\mathcal{L}_2$ -gain performance analysis," *Robotics and Autonomous Systems*, vol. 66, pp. 64–74, 2015.
- [11] D. Lee and K. Y. Lui, "Passive configuration decomposition and passivity-based control of nonholonomic mechanical systems," *IEEE Transactions on Robotics*, vol. 33, no. 2, pp. 281–297, 2017.
- [12] N. Li, P. Borja, J. M. A. Scherpen, A. van der Schaft, and R. Mahony, "Passivity-based trajectory tracking and formation control of nonholonomic wheeled robots without velocity measurements," *IEEE Transactions on Automatic Control*, vol. 68, no. 12, pp. 7951–7957, 2023.
- [13] M. Cui and Y. Wei, "Passivity-based safe maneuvering control of mechanical systems with input constraints," *IEEE Access*, vol. 13, pp. 113171–113178, 2025.
- [14] H. Wu, S. Wang, Y. Xie, H. Li, S. Zheng, and L. Jiang, "Adaptive abrupt disturbance rejection tracking control for wheeled mobile robots," *IEEE Robotics and Automation Letters*, vol. 9, no. 9, pp. 7787–7794, 2024.
- [15] H. Wu, S. Wang, H. Li, Y. Xie, S. Zheng, and S. Q. Xie, "Adaptive fault-tolerant control of wheeled mobile robots with multiple actuator faults and saturation," *IEEE Robotics and Automation Letters*, vol. 10, no. 4, pp. 4156–4163, 2025.
- [16] X. Wang, W. Zhao, C. Wang, X. Zhou, and Z. Luan, "Robust path tracking control of 4WIS-4WID vehicle considering model mismatch uncertainty and actuator fault," *IEEE Transactions on Automation Science and Engineering*, vol. 23, pp. 1–14, 2026.
- [17] Y. Ma, L. He, T. Song, and D. Wang, "Adaptive path-tracking control with passivity-based observer by port-hamiltonian model for autonomous vehicles," *IEEE Transactions on Intelligent Vehicles*, vol. 8, no. 8, pp. 4120–4130, 2023.
- [18] Y. Ma, J. Chen, J. Wang, Y. Xu, and Y. Wang, "Path-tracking considering yaw stability with passivity-based control for autonomous vehicles," *IEEE Transactions on Intelligent Transportation Systems*, vol. 23, no. 7, pp. 8736–8746, 2022.
- [19] X. Liu, W. Wang, X. Li, F. Liu, Z. He, Y. Yao, H. Ruan, and T. Zhang, "MPC-based high-speed trajectory tracking for 4WIS robot," *ISA Transactions*, vol. 123, pp. 413–424, 2022.
- [20] M.-H. Lee and T.-H. S. Li, "Kinematics, dynamics and control design of 4WIS4WID mobile robots," *The Journal of Engineering*, vol. 2015, no. 1, pp. 6–16, 2015.
- [21] B. Čaran, V. Milić, M. Švaco, and B. Jerbić, "Optimal control-based algorithm design and application for trajectory tracking of a mobile robot with four independently steered and four independently actuated wheels," *Actuators*, vol. 13, no. 8, 2024.
- [22] R. Fierro and F. Lewis, "Control of a nonholonomic mobile robot using neural networks," *IEEE Transactions on Neural Networks*, vol. 9, no. 4, pp. 589–600, 1998.
- [23] N. Sarkar, X. Yun, and V. Kumar, "Control of mechanical systems with rolling constraints: Application to dynamic control of mobile robots," *The International Journal of Robotics Research*, vol. 13, no. 1, pp. 55–69, 1994.
- [24] J. Chen, C. Wu, G. Yu, D. Narang, and Y. Wang, "Path following of wheeled mobile robots using online-optimization-based guidance vector field," *IEEE/ASME Transactions on Mechatronics*, vol. 26, no. 4, pp. 1737–1744, 2021.
- [25] Y. Kanayama, Y. Kimura, F. Miyazaki, and T. Noguchi, "A stable tracking control method for an autonomous mobile robot," in *Proceedings., IEEE International Conference on Robotics and Automation*, 1990, pp. 384–389 vol.1.
- [26] V. Milić, J. Kasać, and M. Lukas, "Min–max optimal control of robot manipulators affected by sensor faults," *Sensors*, vol. 23, no. 4, 2023.
- [27] J. Kasać, T. Žilić, V. Milić, A. Jokić, and M. Lobrović, "Robust decentralized global asymptotic tracking control of a class of nonlinear mechanical systems," in *2016 American Control Conference (ACC)*, 2016, pp. 4731–4736.
- [28] H. K. Khalil, *Nonlinear Systems*. Upper Saddle River, New Jersey: Prentice-Hall, 2002.